RSC Advances

ROYAL SOCIETY OF CHEMISTRY

www.rsc.org/advances

A table of contents entry

Synthesis of carbohydrate polymer encrusted gold nanoparticles using bacterial exopolysaccharide: A novel and greener approach

Ganesan Sathiyanarayanan[a], Venkatasamy Vignesh[b], Ganesan Saibaba[c], Annadurai Vinothkanna[d], Krishnamoorthy Dineshkumar[e], Madepalli Byrappagowdu Viswanathan[a], Joseph Selvin[f]*

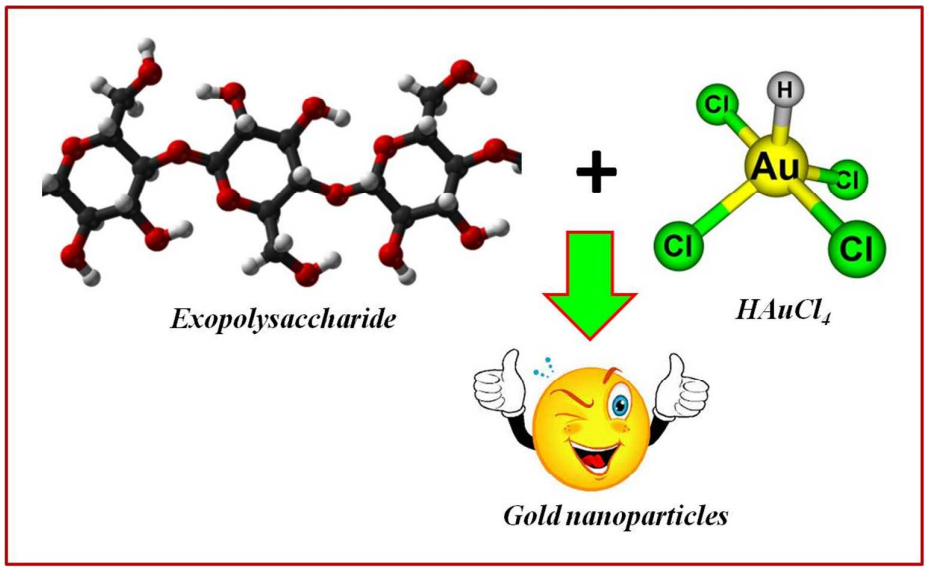

A novel report on synthesis of gold nanoparticles using bacterial exopolysaccharide and synthesized nanocrystals (5–20 nm) were capped with polysaccharide layer.

Synthesis of carbohydrate polymer encrusted gold nanoparticles using bacterial exopolysaccharide: A novel and greener approach

Ganesan Sathiyanarayanan[a], Venkatasamy Vignesh[b], Ganesan Saibaba[c], Annadurai Vinothkanna[d], Krishnamoorthy Dineshkumar[e], Madepalli Byrappagowdu Viswanathan[a], Joseph Selvin[f]*

[a]*Department of Plant Science, School of Life Sciences, Bharathidasan University, Tiruchirappalli 620024, Tamil Nadu, India.*

[b]*Laboratory of Aquabiotics & Nanoscience, Department of Animal Science, School of Life Sciences, Bharathidasan University, Tiruchirappalli - 620024, Tamil Nadu, India.*

[c]*Centre for Pheromone Technology, Department of Animal Science, School of Life Sciences, Bharathidasan University, Tiruchirappalli - 620024, Tamil Nadu, India.*

[d]*Department of Industrial Biotechnology, School of Life Sciences, Bharathidasan University, Tiruchirappalli - 620024, Tamil Nadu, India.*

[e]*Molecular Genetics Lab, Department of Genomic Science, School of Biological Sciences, Central University of Kerala, Kasaragod - 671328, Kerala, India.*

[f]*Microbiology Programme, Pondicherry University, R.V. Nagar, Kalapet, Puducherry - 605 014, India.*

*To whom correspondence should be addressed. Tel: 91-413-2655358; Fax: 91-413-2655734**.**
E-mail: *josephselvinss@gmail.com*

Abstract

In the present study, a marine sponge-associated endosymbiotic bacterium *Bacillus megaterium* MSBN04 was evaluated for exopolysaccharide (EPS) production. The production process was optimized by central composite design (CCD). The productivity was increased up to 5.62 g L^{-1} with sucrose as sole carbon source. The secreted EPS was characterized by NMR analysis and confirming the presence of monosaccharide units such as α-$_D$-glucose and α-$_D$-galactose, which further confirms that the secreted EPS is a heteropolysaccharides. The purified EPS showed considerable flocculating activity (45.41%) with 4 mg l^{-1} of EPS. Using EPS as reducing and stabilizing agent, Gold nanoparticles (AuNPs) were synthesized. The synthesized AuNPs (5-20nm) were in spherical crytalline nature and capped with EPS layer and were characterized by Transmission electron microscopy (TEM) and X-ray diffraction (XRD) analysis. The synthesis of AuNPs was depending on the concentration of EPS. The synthesized AuNPs showed significant antibacterial activity against clinical pathogenic bacteria. Hence EPS-mediated synthesis of AuNPs is an alternative approach to chemical synthesis and thus become an environmental benign greener and economical approach.

Keywords

Exopolysaccharide, Optimization, *Bacillus megaterium*, Gold nanoparticles, Antimicrobial activity

1. Introduction

The demand of biopolymers for industrial applications has led to increased attention in the microbial exopolysaccharides (EPSs) production. The EPSs are long chain branched polysaccharides containing recurring units of the sugar moieties which are secreted into the surrounding medium during the growth of bacteria.[1] Due to unique physical and chemical properties, the bacterial EPSs are widely used in the different industrial sectors as bioabsorbants, bioflocculants, encapsulation materials, drug carriers, ion exchange resins and emulsifying agents.[2, 3] The EPSs are also used as candidates of anti-tumor, anti-viral, and anti-inflammatory agents and also possess indirect effect on colony stimulating factor synthesis in medical field.[4, 5] Nowadays, a major importance has been laid on the search for novel form of EPSs and a wide variety of microbial strains have been identified to produce exopolysaccharides with different compositions and viable properties. The different exopolysaccharides have been comprehensively studied and being currently marketed as commercial products include xanthan, gellan, alginates, cellulose, hyaluronic acid and succinoglycan from various bacterial strains.[6]

Synthesis of gold nanoparticles (AuNPs) which were connected with biomolecules has afforded immensely in medicinal applications such as drug-delivery, gene transfer, bioprobes in cell and tissue engineering.[7] The synthesis of AuNPs through chemical method is now being slowly replaced by environment friendly biological approaches.[8] Among the various biological methods, microorganisms like bacteria, yeast and fungi, are known to reduce inorganic materials either intra- or extra-cellular conditions.[9] However, the actual mechanism of the biosynthesis of AuNPs by different microorganisms and their stabilization via charge capping is poorly understood.

The Polysaccharides are having the hydroxyl groups, a hemiacetal reducing end, and other functionalities that can play important roles in both reduction and the stabilization of inorganic nanoparticles.[10] Over the years, the polysaccharides isolated from plants and animal sources were used as reducer and stabilizer for the synthesis of inorganic nanoparticles.[11–12] They can also be applied for high-performance nanomaterial synthesis, as they produce a range of fluid crystals in aqueous solutions. Therefore, we decided to investigate bacterial EPS for the synthesis of polymer encrusted gold nanocrystals and the EPS-mediated processes are completely greener and productive one. The production of EPS is exclusive as diverse polysaccharides with different biological properties can be produced upon different strains. Due to this, the huge numbers of microbial strains are being evaluated to find out novel EPSs for commercial applications. Currently, marine sponge-associated bacteria are recognized as a rich source of biological macromolecules that are of potential interest towards various industrial applications.[13] Therefore, it is presumed that extensive research on sponge-associated endosymbionts would provide to be a remarkable source of bacterial EPSs. To the best of our knowledge, this is the first report on bacterial EPS based synthesis of carbohydrate polymer encrusted gold nanoparticles. Hence, the present study intended to isolate and characterize the EPS producing novel strains from marine sponges and followed by the production and characterization of EPS from *Bacillus megaterium* MSBN04. Further it is used to synthesize the polymer encrusted AuNPs and the synthesized AuNPs were characterized by UV-spectroscopy, FT-IR, XRD, and TEM analysis.

2. Experimental

2.1 Microorganism, media and culture conditions

The bacterial strain, *Bacillus megaterium* MSBN04 (GenBank ID: HQ874436)[13] was isolated from a marine sponge *Spongia officinalis*, and deposited in Microbial Type of Culture Collection, IMTECH, India under the accession no, MTCC 11946. The strain MSBN04 was cultured at 30 ˚C for two days on a Zobell marine agar M384 (Himedia) and then stored at 4 ˚C, which was sub-cultured for every 2 months interval. The production of EPS was screened by nitrogen deficient medium and the composition of screening medium included glucose, 40 g/L; NH_4NO_3, 1.0 g/L; yeast extract, 0.1 g/L; KH_2PO_4, 0.3 g/L; K_2HPO_4, 0.3 g/L; $MgSO_4.7H_2O$, 0.1 g/L; $MnSO_4.4H_2O$, 0.1 g/L; $CaCO_3$, 0.4 g/L; NaCl, 0.05 g/L and tryptone, 0.1 g/L with the initial pH 7.0 ± 0.2. MSBN04 strain was inoculated in 500 ml Erlenmeyer flasks containing 200 ml of screening medium and incubated in a shaker at 150 rpm for 72 h at 30 ˚C. After incubation, the cell free supernatant (CFS) was collected and checked for EPS production. All chemicals used in this study were of analytical grade.

2.2 Optimization and production of EPS from *B. megaterium* MSBN04

The strain MSBN04 was inoculated into culture medium containing glucose, 10 g/L; yeast extract, 0.5 g/L; KH_2PO_4, 0.2 g/L; NaCl, 0.1 g/L; $MgSO_4.7H_2O$, 0.1 g/L in order to prepare the seed culture for the fermentation process. The initial production of the EPS was performed in 500 ml Erlenmeyer flasks containing 250 mL production medium with 25 mL of seed culture. The composition of the production medium was as follows: sucrose, 20 g/L; yeast extract, 2.5 g/L; NH_4Cl, 1.5 g/L; $MgCl_2$, 0.2g/L; KH_2PO_4, 1.0 g/L; K_2HPO_4, 3.0 g/L and NaCl, 15.0 g/L. The initial pH was adjusted to 6.8 ± 0.2. The inoculated flasks were incubated with 150 rpm agitation at 30 ˚C. The optimal pH (5.0–10.0) for EPS production was analyzed with production medium. The strain was incubated at different temperatures

(20, 25, 28, 30, 37, 45 and 50 ˚C) and NaCl concentrations (1.0–8.0%). The effect of different carbon sources, nitrogen sources and metal ions on cell growth and EPS production were tested after 42 h of incubation. Process optimization was performed with response surface methodology (RSM) to optimize the concentration of medium ingredients to improve EPS production. Four independent factors (sucrose, NH_4Cl, K_2HPO_4, and NaCl) were selected from classical optimization that significantly affected EPS production. A central composite design (CCD) was obtained from the Design-Expert software (State-Ease, Inc., Minneapolis, USA, trial version 8.0.7.1) and was applied to elucidate the interactions of these independent factors on the EPS production. An experimental design of 32 experiments (5-level-4-factorial) with six central points were formulated and the experiments were conducted in 500 mL Erlenmeyer flasks containing 200 mL of media was prepared according to the design and inoculated with 10 mL of seed culture. The flasks were incubated at 30 ˚C with 200 rpm of agitation. All experiments were performed in triplicates. In addition, the average EPS production was used as the dependent variable. Dry weight of the EPS (g/L) was studied as response at the end of 42 h incubation. The 3-D contour graphs were created to understand the interaction of different variables (factors) and the graphs were used to evaluate the optimized components of the medium, which influences the responses.[14]

2.3 Extraction and purification of EPS

The culture volume of 250 mL was centrifuged at 12, 000 × g for 10 min at 4 ˚C. The cell pellet was freeze-dried and weighed. The cell-free supernatant was subjected to thermal treatment (80 ˚C, 1h) to inactivate bacterial enzymes that might cause EPS degradation during the following purification steps. For the purification of EPS, ice cold absolute ethanol was added into the cell-free supernatant at the ratio of 2:1 (V/V) in a 500 mL of Erlenmeyer flasks and kept at 4 ˚C for overnight. The exopolymeric precipitate was collected by high dry

centrifugation at 14,000 × g for 15 min at 4 ˚C. The precipitate was washed with 70–100% ethanol-water mixtures. After ethanol-water washing for thrice, the precipitates which were combined and dried in a desiccator and stored at room temperature till needed. The EPS was re-dissolved in distilled water and dialyzed at 4 ˚C for 12 h against de-ionized water for desalting. Excessive water content was removed under vacuum and lyophilized precipitate was stored at room temperature until physical and chemical analyses performed. To get purified polymer, the freeze-dried precipitate was dissolved in 50 mM phosphate buffer (pH-7.0) containing 0.5 M NaCl and gel-filtered through the phenyl sepharose column (AKTA prime plus protein purification system, GE Healthcare, Sweden). The dissolved sample was eluted by same buffer with flow rate of 2 mL/min. The eluted EPS fraction was freeze-dried using freeze drier for further analyses.

2.4 Characterization of EPS

The UV-Visible spectrum of purified EPS was recorded between 200 and 800 nm using a spectrophotometer. Purified 0.75 mg of EPS was carefully mixed with potassium bromide (KBr) and dried. The dried EPS sample was analyzed using Fourier Transform Infrared Spectrophotometer (FT-IR) (Perkin Elmer, USA) with a resolution of 4 cm^{-1} in 4000-400 cm^{-1} region.[15] The chemical composition of the EPS was investigated by carbohydrate assay and thin layer chromatography (TLC). For chemical analyses, EPS was hydrolyzed with 2 N HCl for 140 min at 100 ˚C in ampoules flushed with N_2 before sealing and thereafter the solution was neutralized with NaOH solution. After cooling, the sample was freeze-dried and dissolved in Milli-Q water (100 µL). The hydrolyzed sample was spotted onto silica gel coated glass TLC plates. The solvent system such as mixture of acetonitrile, ethyl acetate, ethanol and water (85:25:25:15) was used for the separation of monosaccharide moieties which are present in the polysaccharide. The fractions were

visualized by heating the TLC glass plates after spraying with H_2SO_4 (5%, v/v) in ethanol. The control tests were performed with commercial sugars as standards for the identification sugar composition in the bacterial EPS. The lyophilized crude EPS was dissolved in ultrapure Milli-Q water (0.1 g L^{-1}) and total carbohydrate contents were assayed by phenol sulphuric acid method with glucose as standard.[16] The protein content was calculated with bovine serum albumin (BSA) as standard using Bradford assay.[17] Sulfated sugars were determined by measuring the amount of sulfate content using K_2SO_4 as standard.[18] Nuclear magnetic resonance (NMR) spectra were obtained using a Bruker Avance 400 MHz spectrometer (Bruker Co., Billerica, MA) with a 5-mm inverse probe. Proton spectra were run at at 25 ˚C, while carbon spectra were obtained at 25 ˚C. EPS of the *B. megaterium* MSBN04 dissolved in DMSO-d_6 at concentrations of 5 mg ml^{-1} (for ^{1}H NMR) and 20 mg ml^{-1} (for ^{13}C NMR). Structure and arrangement of secreted EPS was analyzed by Scanning Electron Microscope (SEM).

2.5 Determination of flocculating activity of EPS

The flocculating activity was predicted using a solution of kaolin clay as the suspended solid. Briefly, 5.0 ml of 1% (w/v) $CaCl_2$ and 0.2 ml of EPS (5 mg l^{-1}) were added into 95 ml of kaolin suspension (5.0 g/l, pH 8.0). The mixture was stirred for 4 min and then allowed to incubate for 5 min at 28 ˚C. The optical density (OD) of the aqueous phase was measured at 550 nm with a UV-vis Spectrophotometer. A control was prepared in the same way except EPS and the flocculating activity was measured according to the following mathematical equation.[19]

$$\text{Flocculating activity} = \frac{B-\text{A}}{\text{A}} \times 100\% \quad (1)$$

Where A and B are the OD of the EPS and the control respectively. The effects of EPS concentration, temperature and pH of the solution on flocculating activity were also

198 examined. The concentration of EPS varied from 1–8 mg l^{-1}. The pH of the kaolin
199 suspension was adjusted using 1M NaOH and 1N HCl in the pH range of 5–12.0. The
200 temperature of kaolin suspension was changed in a water bath in the range of 5–60˚C.
201
202 **2.6 Synthesis of gold nanoparticles using EPS**
203 MSBN04 was freshly inoculated in statistically optimized production medium which
204 contains sucrose, 40 g/L; yeast extract, 2.5 g/L; NH_4Cl, 2.0 g/L; $MgCl_2$, 0.2g/L; KH_2PO_4, 1.0
205 g/L; K_2HPO_4, 5.0 g/L and NaCl, 20 g/L. The initial pH was adjusted to 6.8 ± 0.2. The flasks
206 were incubated at 30 ˚C for 72 h with 200 rpm. After incubation, the cultured broth was
207 centrifuged at 8000 rpm for 10 min. The bacterial EPS was purified from culture supernatant
208 and was used for the synthesis of AuNPs. For the synthesis of AuNPs, chloroauric acid
209 ($HAuCl_4$) (HiMedia) was prepared at the concentration of 10^{-3} M (1 mM) with pre-sterilized
210 Milli-Q water. A quantity of 5 mg/mL solution of EPS was mixed with 30 ml of 10^{-3} M (1
211 mM) of $HAuCl_4$ in a 100 mL of Erlenmeyer flasks for the synthesis of AuNPs. $HAuCl_4$ was
212 taken in similar quantity without adding EPS solution as main control. The flasks were tightly
213 covered with aluminum foil in order to avoid photo reduction of gold ions and incubated at
214 room temperature under dark condition. The observations were recorded at every 12 h
215 interval. The extracellular synthesis of AuNPs was monitored by visual inspection of flasks
216 for the change in color of the EPS from a clear colorless solution to red. The synthesized
217 nanoparticles were collected by high speed centrifugation (20000 × g for 20 min), washed
218 with Milli-Q water and dialyzed against Milli-Q water to get pure AuNPs. Synthesis of
219 AuNPs was optimized with different concentrations of EPS and gold precursor such as
220 $HAuCl_4$.
221
222

2.7 Characterization of synthesized AuNPs

The reaction mixture incubated at room temperature was scanned at 0 h onwards with spectral range between 200 to 800 nm wave lengths with UV-visible Spectrophotometer (Perkin Elmer, USA). The reaction mixtures were scanned under the same wavelengths up to 60 days. The synthesized AuNPs were characterized by FT-IR, X-ray diffraction analysis (XRD) and Transmission electron microscopy (TEM) analysis. The size of the AuNPs was measured and average particle sizes and distribution were determined. Zeta potentials of AuNPs were also determined to know about their colloidal stability.

2.8 Antimicrobial Activity of EPS based synthesized AuNPs

Antimicrobial activity of the synthesized AuNPs was assessed by standard disc and well diffusion method according to National Committee for Clinical Laboratory Standards (NCCLS). Mueller-Hinton agar (MHA) plates were inoculated with with 12 h old broth cultures of the test organisms such as six MTCC bacteria and three clinical pathogens to create a confluent lawn of bacterial growth. For well diffusion, the wells of 6 mm diameter were made on the Muller Hinton agar (MHA) plates. 50 µL of AuNPs solution containing 10, 20, 40 and 100 µg/mL of AuNPs were loaded in each well. In disc method, paper disc at 6 mm dimension was impregnated with AuNPs at different concentrations (20, 40 and 100 µg/mL). The antibacterial activity of pure EPS and chemically synthesized gold nanoparticles were also checked along with EPS stabilized AuNPs as control experiments. Sodium citrate was used as reducing agent to prepare chemically synthesized gold colloidal solution for the antibacterial activity. The agar plates were incubated at 37 ˚C for 24 h and the inhibitory pattern was determined by measuring the diameter of the zone of inhibition around the disc and well (in mm). The experiments were repeated thrice and the average values were calculated.

2.9 Statistical analysis

All the experiments were carried out in thrice. The spectral pattern and photograph of AuNPs were selected from one of the replicate samples. Statistical analysis (means) of the experimental data was carried out by MS Excel 2007 and the Design Expert Software (State-Ease, Inc., Minneapolis, USA, version 8.0.7.1) was used for polynomial analysis and to plot response surfaces. ANOVA was used to estimate the statistical parameters for optimization experiments.

3. Results and discussion

3.1 Production of EPS from MSBN04

The production of EPS by *B. megaterium* MSBN04 occurred only in the late log phase of bacterial growth. The optimal pH, temperature, and NaCl for EPS production by MSBN04 were determined and the maximum EPS (g L^{-1}) production was attained at pH 7.5 (4.902 ± 0.31), 30 ˚C (4.512 ± 0.22) with addition of 3–4% of NaCl (5.118 ± 0.33), respectively. Effect of carbon sources on cell growth and EPS production by *B. megaterium* was investigated and sucrose (30 g L^{-1}) was found to be the best carbon source for the growth and EPS production (Table 1). Inorganic nitrogen sources such as NH_4Cl and NH_4NO_3 were obviously better nutrients for both cell growth and EPS production. In this study, the EPS production was strongly affected by various metal ions, which are present in the production medium. The K_2HPO_4 was found to be the best for EPS production and increased concentration of $MgCl_2$ also significantly enhanced the EPS yield and growth of *B. megaterium* MSBN04.

273 **Table 1** Effect of carbon, nitrogen sources, and metal ions on the production of
274 exopolysaccharide.

Medium Ingredients	Growth of MSBN04 (OD_{600})	EPS production (g L^{-1})
Carbon source (%)		
Glucose	1.435±0.06	4.283±0.51
Sucrose	1.637±0.02	5.223±0.04
Mannitol	1.413±0.17	3.233±0.10
Fructose	1.506±0.01	4.050±0.07
Lactose	1.263±0.03	2.103±0.04
Arabinose	1.421±0.04	3.470±0.29
Xylose	1.340±0.00	2.173±0.23
Nitrogen source (%)		
Peptone	1.299±0.03	3.273±0.25
Beef extract	1.401±0.01	3.467±0.10
Yeast extract	1.529±0.06	4.420±0.30
Casein	1.277±0.01	2.213±0.11
Urea	1.267±0.12	1.867±0.11
NH_4Cl	1.631±0.04	5.140±0.11
NH_4NO_3	1.593±0.01	4.257±0.16
Metal ions (%)		
$MgCl_2$	1.411±0.01	3.623±0.23
K_2HPO_4	1.600±0.02	5.046±0.13
KH_2PO_4	1.267±0.12	2.493±0.30
$MnCl_2$	1.309±0.02	2.266±0.25
$FeCl_2$	1.221±0.02	1.816±0.05
$CaCl_2$	1.306±0.01	2.316±0.21
KCl	1.409±0.02	3.350±0.35

275 The results are represented as Mean ± SD and all the values are significant at the level of
276 $P<0.05$ (n=3).
277
278
279

3.2 CCD optimization of EPS production from MSBN04

Response surface methodology (RSM) is a statistical tool for optimizing medium components and their interactive concentrations to improve the productivity. Based on classical optimization, the most significant variables such as sucrose, NH_4Cl, K_2HPO_4 and NaCl were identified using one factor at a time experiment. The production medium was optimized by CCD with six central points. The overall second-order polynomial equation for EPS production was given below:

$$\text{EPS Yield (Y)} = +5.62 + 0.63 \times A - 0.14 \times B + 0.12 \times C + 0.080 \times D + 0.072 \times A \times B + 0.093 \times A \times C - 0.15 \times A \times D + 0.041 \times B \times C - 0.084 \times B \times D - 0.15 \times C \times D - 0.88 \times A^2 - 0.66 \times B^2 - 0.74 \times C^2 - 0.96 \times D^2 \quad (2)$$

Where *Y* was the response, i.e. the flocculant content, and *A, B, C* and *D* were the coded terms for the four test vaiables, i.e. sucrose, NH_4Cl, K_2HPO_4 and NaCl respectively. The statistical significance of the model equation was calculated by F-test for analysis of variance (ANOVA), which indicates that the regression is strongly significant at 99% (P<0.0500) confidence level. In this case A, B, C, AD, CD, A^2, B^2, C^2 and D^2 are significant model terms. P-values indicate the significance of each coefficients and it is important to understand the pattern of the mutual interaction among variables. The smaller the magnitude of the *P*, the larger is the corresponding coefficient which shows that the obtained statistical model is more significant and stronger the relationship between the variables. The ANOVA for EPS production exhibited the model *F*- value of 70.22 that implies the model is significant at Prob>*F*- value which was <0.0001. There is only a 0.01% chance that a "Model F-value" this large could occur due to noise (Table 2). "Adeq Precision" measures the signal (response) to noise (deviation) ratio. The obtained ratio of 26.545 indicates an adequate signal in the case of optimization (medium) of EPS production.

Table 2 ANOVA analysis of CCD optimization of exopolysaccharide production by *B. megaterium* MSBN04.

Source	Sum of Squares	df	Mean Square	F Value	p-value Prob > F
Model	63.72	14	4.55	70.22	<0.0001**
A-Sucrose	9.49	1	9.49	146.38	<0.0001**
B-NH_4Cl	0.44	1	0.44	6.79	0.0199*
C-K_2HPO_4	0.36	1	0.36	5.52	0.0329*
D-NaCl	0.16	1	0.16	2.39	0.1426
AB	0.083	1	0.083	1.28	0.2765
AC	0.14	1	0.14	2.14	0.1641
AD	0.36	1	0.36	5.51	0.0331*
BC	0.026	1	0.026	0.41	0.5329
BD	0.11	1	0.11	1.76	0.2048
CD	0.35	1	0.35	5.42	0.0344*
A^2	21.26	1	21.26	327.93	<0.0001**
B^2	12.10	1	12.10	186.60	<0.0001**
C^2	14.88	1	14.88	229.57	<0.0001**
D^2	25.36	1	25.36	391.26	<0.0001**
Residual	0.97	15	0.065		
Lack of Fit	0.97	10	0.097		
Pure Error	0.000	5	0.000		
Core total	64.70	29			

*Significant; **Most significant; df, degrees of freedom

The R^2 value of 0.9850 which is closer to 1 shows the model to be stronger which can better predict the response and the model could explain 98% of the variability in the production of EPS. The model so obtained for EPS was adequate as depicted from the low *F*-value, insignificant 'lack of fit' and R^2 closest to unity, thus elucidating the significance of responses could be explored by this model. The high value of adjusted R^2 (0.9709) further supports the accuracy of the model. Three dimensional response surface curves were plotted to study the interaction of substrates on the EPS production. Interactions of AC, AD and CD would contribute positively for the EPS production which means CD and AD are statistically significant and AC interaction is not statistically significant but still its exhibit a smaller *P* value than other interactions (Table 2 & Fig.1). The 3-D response surface graphs in Fig.1, which depict the interactions between the two factors (variables) by keeping the other

variables at their zero levels. A circular contour plot under the response surfaces indicates that the interaction between the corresponding variables can be ignored, while an elliptical or saddle nature of the contour plot suggests that the interaction between the corresponding variables is significant. On the other hand, the interactive model terms AB, BC, and BD and did not depict significant impacts on the EPS production (Table 2 & Fig.S1), but there is a considerable increase in the productivity when these independent variables present altogether in the production medium. The "Pred R-Squared" of 0.9134 is in reasonable agreement with the "Adj R-Squared" of 0.9709. During the RSM experiments, nitrogen source *i.e.* NH_4Cl was found to be limiting nutrient for the production of EPS. The maximum EPS production predicted is 5.60 g L^{-1}, and the actual production obtained with optimized medium was 5.62 g L^{-1}, which is in close agreement with the model prediction as obtained and from the response study, it is obvious that all substrates have significant impacts on the EPS production.

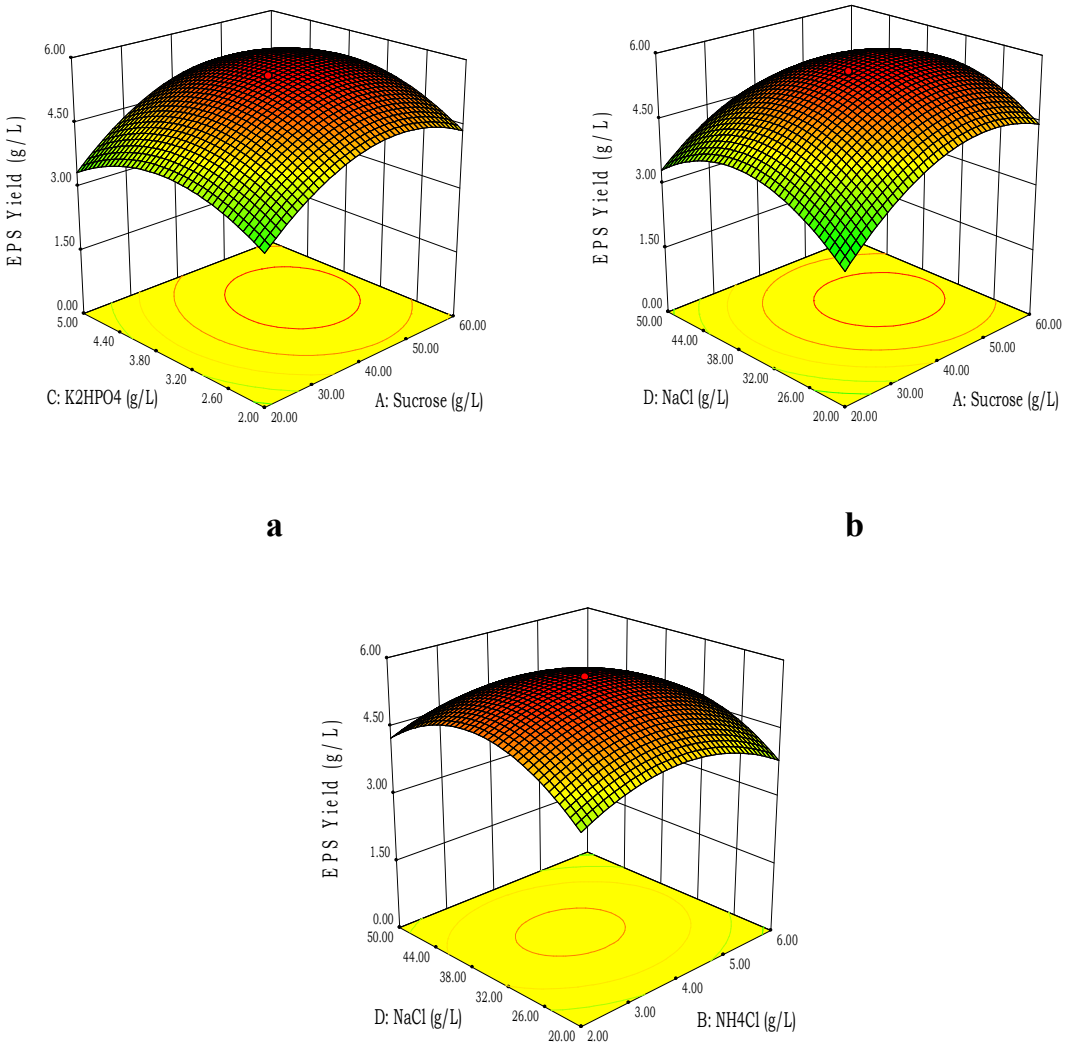

Fig. 1 Three dimensional response surface graphs obtained from central composite design. The figure shows the interactive effects of different factors (A, B, C & D) on the production of EPS by the sponge bacterium MSBN04. a) Interaction between Sucrose (A) and K_2HPO_4 (C); b) Interaction between Sucrose (A) and NaCl (D); c) Interaction between NH_4Cl (B) and NaCl (D).

3.3 Characterization of EPS

UV- Vis spectroscopy analysis showed the major wavelength area of absorption peak between 200 and 240 nm owing π-π^* transitions, which exhibit functional groups like carboxyl, carbonyl and amine.[20] In addition, a minor peak at around 270-280 nm was observed, which is typical for π-π^* transitions in aromatic or poly-aromatic compounds present in the most conjugated molecules such as proteins. The EPS UV spectrum was given with AuNPs UV spectrum in Fig. 3a. The FT-IR analysis showed diverse range of absorption peaks from 3442 to 463 cm^{-1} (Fig. 2).

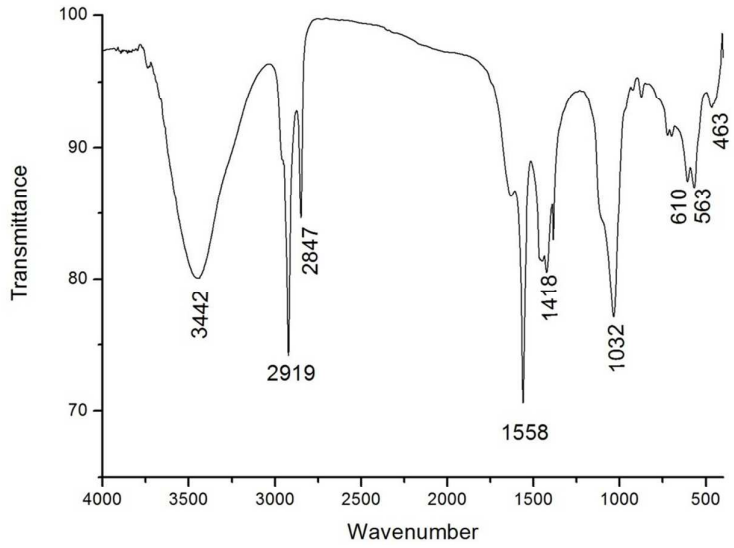

Fig. 2 FT-IR spectrum of purified EPS. FT-IR shows peaks at 563–875 cm^{-1} confirms the presence of saccharide moieties.

The purified EPS contains a many hydroxyl groups (O–H) stretching frequencies, which showed broad absorption peak around 3442 cm^{-1}, which suggested that purified polymer is a polysaccharide.[21] Two strong absorption peaks at 2919 and 2846 cm^{-1}, assigned to C–H asymmetric stretch and C–H symmetric stretch of CH_2 and CH_3 groups, respectively.

The strong absorption band at 1558 (C–O–H) and small peak at 1627 cm^{-1} (C=O & C–N) indicates the archetypal IR absorption of polysaccharide.[22] A symmetrical stretching band at 1418 cm^{-1} showed the presence of carboxyl groups. The strong absorption peak at 1032 cm^{-1} corresponds to the presence of carbohydrates.[23] Peaks around 563–875 cm^{-1} gives clue about the presence of saccharide moieties. A comparison of functional groups revealed that the purified EPS contained different functional groups and were more complex than other bacterial EPSs were reported earlier.[24] The FTIR spectrum of EPS from *B. megaterium* MSBN04 exhibited major functional groups such as carboxyl and hydroxyl groups which may act as a receptor for divalent cations (Ca^{2+}) during emulsification and flocculating activity.[25] The composition of EPS was analysed by TLC and the results showed two apparent sugars spots which were identified as glucose and galactose based on their retention factor (Rf). The presence of two different monosaccharides suggests that the EPS is a hetero-polysaccharide polymeric compound. Similarly, two monomeric sugar moieties such as glucose and galactose were identified in EPS from *Lactobacillus fermentum* TDS030603 using TLC.[26] The growth medium ingredients especially carbon source is mainly responsible for the composition of bacterial EPSs. The chemical analysis of EPS from MSBN04 revealed a gross variation in chemical composition. The contents of total carbohydrates, protein and sulfate were found to be 353.14, 127.68 and 30.28 mg l^{-1}, respectively. In general, carbohydrate contents of the EPSs were higher than proteins and sulfated content, a feature that was observed with other bacterial EPSs.[21]

NMR characterization of EPS has been done to identify the possible monosaccharide units, which are present in the EPS. ^{1}H-NMR spectrum (Fig. S2a), it was likely to identify two resonances in the region for α-anomeric protons at δ 6.1 and 6.0 ppm as partially resolved doublets. [27, 28, 29] This anomeric proton information reveals that the purified EPS

mainly consists of two types of monosaccharides moieties, which was consistent with the monosaccharide composition perceived by TLC. The two small signals at δ 4.9 and 4.6 ppm (doublet as 4.601, 4.613) should belongs to glucose and these signals may due to reduced end-chain α-$_D$-glucose. A signal at δ 4.7 ppm (doublet as 4.746, 4.732) was assigned to reduced end-chain α-$_D$-galactose. The signals at δ 4.91-4.20 ppm shifts were characteristic of glucose and galactose. ^{13}C-NMR spectra of EPS are shows two main signals in the anomeric region at δ 92.54 and 92.16 ppm (Fig. S2b), and were assigned to the α-$_D$-galactose and (1–6)-linked α-$_D$-glucose residues, respectively. [28, 30] Further, ^{13}C-NMR spectrum appears as doublets but indicating that the same monosaccharide at different locations resulted in anomeric carbon chemical shift. Since, it is both glucose and galactose are epimers. Due to this reason, for an EPS in DMSO-d$_6$ all glucose hydroxyl signals merge into other signal owing to a fast exchange in NMR time scale. According to NMR results, the main constituents of purified EPS are α-$_D$-glucose and α-$_D$-galactose, which was corroborates with the results of the TLC analysis. SEM image shows that the EPS polymer purified from *B. megaterium* MSBN04 is arranged in a complex filamentous form (Fig. 6a). Pure EPS has been subjected for ultra-sonication to make individual particles of EPS, which results the EPS particle size around ~100nm were used for gold nanoparticle synthesis.

3.4 Flocculating activity of EPS

An optimal concentration of EPS for flocculating activity was determined using kaolin clay suspension with constant invariables (EPS, 5 mg l^{-1}; pH, 8.0; Temperature, 28°C). The highest flocculating activity (45.41%) was observed at the concentration of 4.0 mg l^{-1} (Table 3). The EPS was highly stable at alkaline and showed 25.78% of flocculating activity at pH 12.0. The flocculating activity was high at pH 9.0 with 29.14%, it is noteworthy and EPS from MSBN04 can be used for the treatment of high salinity water bodies as

418 bioflocculant. The flocculating activity was also stable (36.53%) at high temperature (60 ˚C).
419 There are few reports shows that the flocculation activity ranging from 50 to 95% [31, 32] and
420 flocculating activity up to 92.07% [3] in the case of using polysaccharide flocculating agent
421 from bacteria. In this study, it has been reported that 45.41% of flocculation activity of EPS
422 produced by *B. megaterium* MSBN04. Upon comparing with existing studies, the yield is
423 neither less or high and it is considered as a moderate. EPS from MSBN04 exhibits
424 flocculating activity at high temperature and high salinity, which envisages its potential use
425 for colloid and cell aggregation purpose, which will be very useful for numerous applications,
426 such as wastewater treatment, food and mining industries. Currently, synthetic (inorganic &
427 organic) flocculants are widely used for commercial applications, but they have low
428 biodegradability and are not shear resistant.[31] In addition, some of them are neurotoxic and
429 cause deleterious effects on human and animal health. To avoid these environmental and
430 public health hazards, naturally occurring bioflocculants, including several bacterial
431 exopolysaccharides are recommended as safe alternatives.[32] Thus, the EPS produced by
432 marine sponge-associated *B. megaterium* MSBN04 might be included among these
433 bioflocculants.

434

435 **Table 3** Effect of EPS concentration, temperature, and pH on flocculation activity

EPS Concentration (mg l^{-1})	Flocculating activity (%)	Temperature (˚C)	Flocculating activity (%)	pH	Flocculating activity (%)
1.0	4.08	5	0.00	5	10.22
2.0	7.92	15	5.13	6	16.05
3.0	20.28	25	11.79	7	20.92
4.0	45.41	28*	20.23	8*	25.67
5.0*	38.02	37	36.04	9	29.14
6.0	42.76	45	37.25	10	28.33
7.0	44.22	50	35.11	11	28.06
8.0	40.08	60	36.53	12	25.78

436 *constant invariables: EPS, 5 mg l^{-1}; pH, 8.0; Temperature, 28 ˚C

437

438 **3.5 Synthesis of AuNPs using bacterial EPS**

439 The AuNPs were synthesized by reducing Au^{+} to Au^{0} with addition of EPS in a
440 solution of $HAuCl_4$ followed by storage at room temperature in the dark. In the presence of
441 EPS, the colorless solution was turned into red color indicating the formation of AuNPs.
442 There was no change in the color of the control mixture without EPS. The synthesis of
443 colloidal AuNPs can regularly be confirmed by measuring the excitation of surface plasmon
444 resonance band, typical of the AuNPs using UV-vis spectrophotometry. Fig. 3a shows that
445 the UV-Vis spectrum of the EPS based synthesized AuNPs after 12 days of incubation. Here
446 EPS alone has considered as a control. The EPS-stabilized AuNPs revealed a solid absorption
447 spectrum and increased intensity around at 560 nm with a broad band, representing the
448 synthesis of AuNPs that varied in shape and size. The absorbance and position of the surface
449 plasmon resonance depends upon the intrinsic factors such as pH, temperature, dielectric
450 properties, size and shape of the particles. There is no absorption peak was detected in the
451 EPSs with $HAuCl_4$ on day 0. It was observed that AuNPs peak remained close to 560 nm
452 even after 60 days of incubation and the plasmon resonance peak could become more widen
453 and the absorption spectrum was slightly shifted to different position. The slight changes in
454 the absorption spectra of the EPS-stabilized AuNPs indicate the presence of well-dispersed
455 nanoparticles in the EPS solution and covered by polysaccharide moieties. This result
456 corroborates with the earlier reports[33], they found that the absorption maxima of
457 polysaccharide stabilized metallic nanoparticles slightly shifted after 30 and 60 days of
458 incubation. The hydrogen bonds present in the polysaccharides provide surface passivation
459 against the agglomeration of metallic nanoparticles. Incubation with different concentrations
460 of EPS resulted in the preparations with the same major peak between 562 and 568 nm,
461 which indicates that similar particle sizes and shapes of AuNPs were produced. No color
462 change and absorbance were seen in the absence of EPS. The peak absorbance intensity

increased with increasing concentrations of EPS, and the maximum absorbance intensity was obtained at 5 mg/mL of EPS concentration (Fig. 3b). The peak with higher intensity also suggested increased AuNPs concentration.[34] The gold precursor $HAuCl_4$ concentration was optimized for the synthesis of AuNPs. The increased concentration of precursor (1.0 mM to 3 mM), lesser the intensity of AuNPs absorbance in UV spectrum analysis and it confirms that the initial concentration 1.0 mM is an optimum concentration for the synthesis of EPS encrusted gold nanocrystals (Fig. S3).

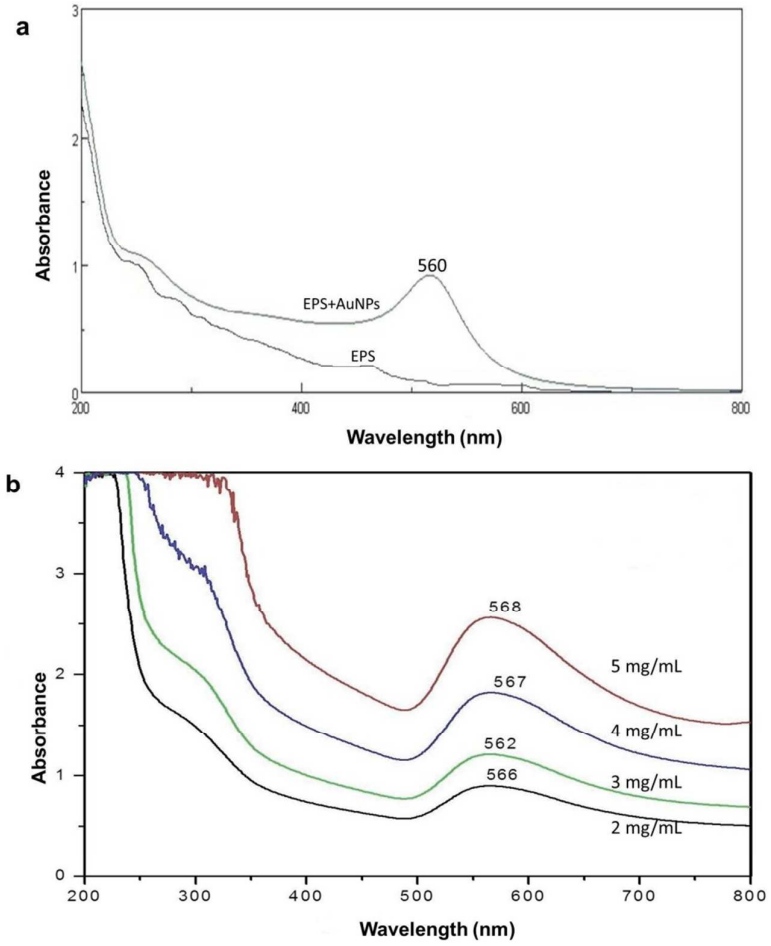

Fig. 3 Synthesis of gold nanoparticles. Biosynthesis of gold nanoparticles (AuNPs) was confirmed by UV-visible spectroscopy. (a) UV-visible absorbance of EPS and AuNPs synthesized by EPS; (b) UV-visible spectrum of AuNPs synthesized with different EPS concentration.

475 **3.6 Characterization of AuNPs**

476 The FT-IR analysis was carried out to identify the possible interaction between gold
477 ions and exopolysaccharide, which could account for the reduction of Au^{+} ions and
478 stabilization of AuNPs. The FT-IR spectra (Fig. 4a) show peaks at 523, 610, 879, 1025, 1384,
479 1578, 2846, 2919 and 3432 cm^{-1}. The peaks at 1025 and 1384 cm^{-1} could be due to the
480 bending vibration of C–O–C groups and the antisymmetric stretching bands of C–O–H
481 groups of polysaccharides and this type of peaks were also observed in pure EPS (1038, 1418
482 cm^{-1}).[35] Two bands at 2919 and 2846 cm^{-1}, assigned to C–H asymmetric stretching and C–H
483 symmetric stretching of CH_2 and CH_3 groups, respectively.[4] The peak at 1578 cm^{-1} could be
484 due to the amide-I protein. Specifically, the peaks at 523, 610 and 879 cm^{-1} ascertain the
485 presence of sugar moieties and more or less the relevant peaks were also observed in
486 extracted EPS (563, 610 and 875 cm^{-1}). A broadly stretched intense peak at around 3432 cm
487 is a characteristic of hydroxyl groups (OH). The FT-IR spectrum of AuNPs exhibited the
488 presence of carboxyl, hydroxyl and methoxyl groups and which were major groups of
489 purified EPS from MSBN04 that could most possibly to form a capping around the AuNPs
490 and stabilizing the nanoparticles in an aqueous solution. The electrostatic attractive forces
491 between polysaccharide (amino sugar moieties) and Au^{+} in solution provide an effective
492 driving force for the synthesis and stabilization of the AuNPs. Thus, in this report, we
493 demonstrated that the synthesis of AuNPs using bacterial exopolysaccharide and this
494 approach is novel and greener. Different plant-derived polysaccharides were used for the
495 synthesis and stabilization of metallic nanoparticles, [12, 36] meanwhile microbial
496 exopolysaccharides have not yet been utilized for the synthesis of colloidal AuNPs. Stability
497 of EPS based colloidal gold solution has been investigated by zeta potential (ζ), which is a
498 measure of the electrostatic potential on the surface of the nanoparticle and is related to the
499 electrophoretic mobility of the colloidal suspension. The overall absorbance of zeta potential

(-29.1mV) (Fig. S4) revealed the incipient instability (from ±10 to ±30mV) nature occurred and the optimization experiments to increase the stability of EPS stabilized AuNPs are currently in progress.

The XRD spectrum of synthesized AuNPs showed the prominent Bragg reflection. The reflections assigned to diffraction from (111), (200), (220) and (311) at the 2 □ of 38.125, 44.278, 64.699, and 77.564, respectively (Fig. 4b). These distinctive XRD spectral peaks arise due to the presence of a face-centered cubic (*fcc*) structure of the gold nanocrystals. The obtained results indicate that the synthesized AuNPs are in the form of colloidal nanocrystals. Amongst the diffraction planes, plane (111) was stronger than other diffraction plans, it might be due to the major orientation of the (111) plane. Similar results were reported for metallic nanoparticles synthesis when plant and bacterial-derived polysaccharides were used.[33]

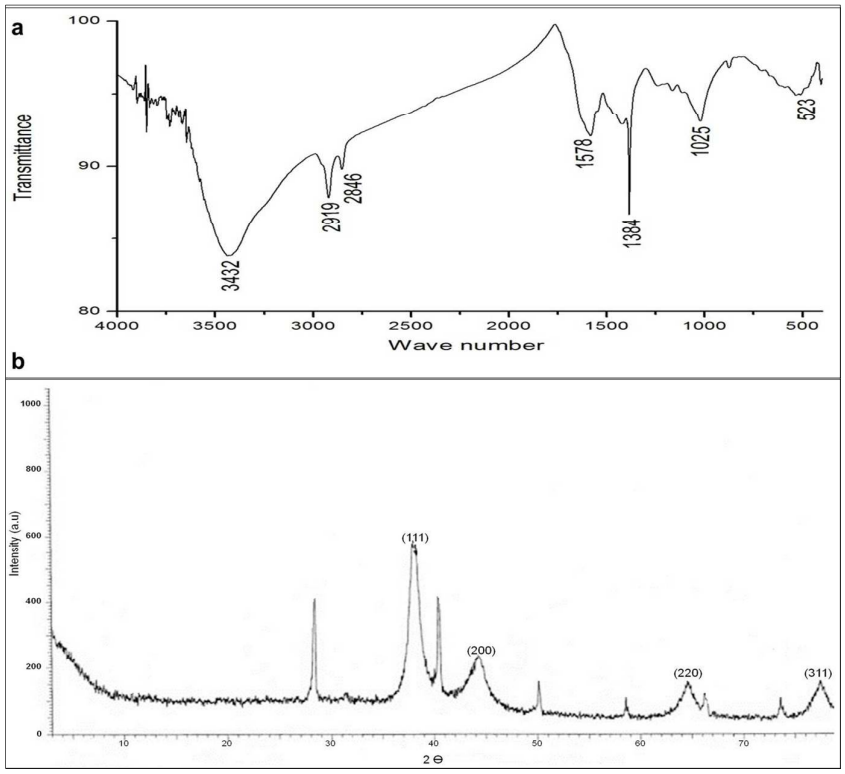

Fig. 4 Characterization of synthesized and EPS stabilized gold nanoparticles. (a) FT-IR spectrum of synthesized AuNPs; (b) XRD spectral pattern of synthesized gold nanocrystals.

The TEM analysis was performed to observe the morphological feature and size of the synthesized AuNPs, and the results are shown in Fig. 5. The TEM images displayed spherical shape gold nanoparticles and the distribution of AuNPs varied in size ranging from 5 to 20 nm with an average size of 10 nm. These sizes are common in AuNPs synthesized by polysaccharides such as heparin and hyaluronic acid.[11, 12] Also a similar result was observed[29] and reported that the silver nanoparticles were synthesized by exopolysaccharide purified from lactic acid bacterium *Lactobacillus rhamnosus* GG ATCC 53103. The low magnification TEM images illustrate the structures of the secreted exopolysaccharide (~100nm) (Fig. 6b). TEM images also exhibit the gold nanoparticles were growing inside of the exopolysaccharide (EPS) matrix and the particles were encrusted with EPS polymer. Moreover, spherical-shaped synthesized AuNPs were capped by bacterial exopolysaccharides, which are clear and visible in the TEM image as a faint thin layer (Fig. 5). This exopolysaccharide coating is mainly responsible for the stabilization of AuNPs, also entraps AuNPs and forms a clump of nanoparticles (Fig. 6b). The result agrees with the findings that[10, 37] polysaccharide moieties were involved in the reduction and stabilization of silver nanoparticles. In addition, spherical shaped AuNPs were reported with an average size of 20 nm using polysaccharide such as dextran as a reducing and surface coating agent for the synthesis of stable, biocompatible AuNPs.[38] The diameters distribution of 100 AuNPs were obtained by particle size analyser and it showed that the range from 3 to 25 nm with mean size of 15 nm. The size and shape of metallic nanoparticles depends on the concentration and type of reducing and stabilizing agents used. Experiments on how to control sizes and shapes of AuNPs synthesized with bacterial exopolysaccharides are currently in progress.

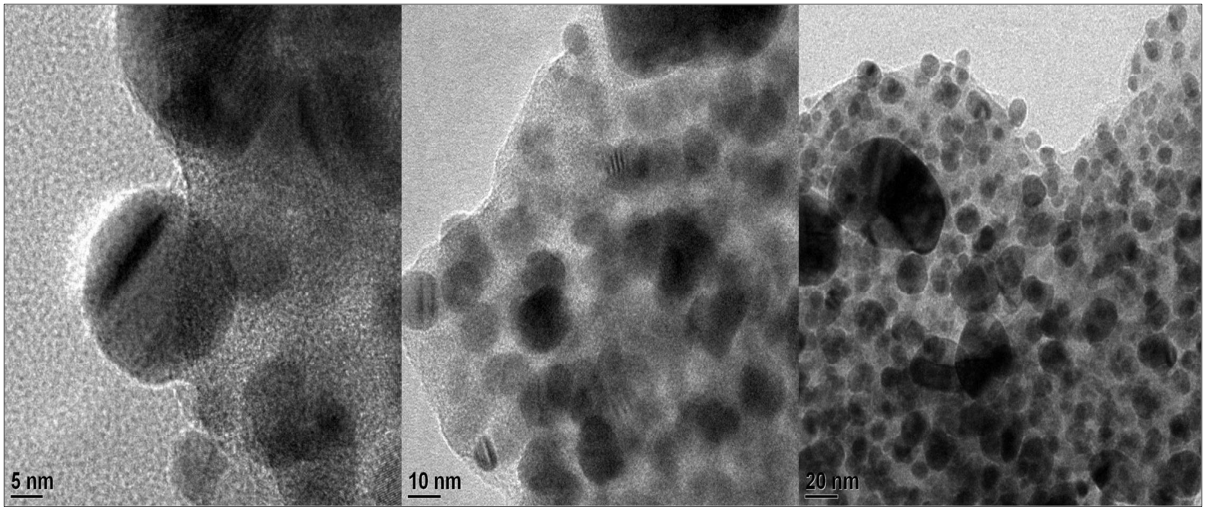

Fig. 5 TEM micrograph of EPS stabilized gold nanoparticles. Different sizes of gold nanoparticles (5-20 nm) were capped by the thin faint layer of EPS.

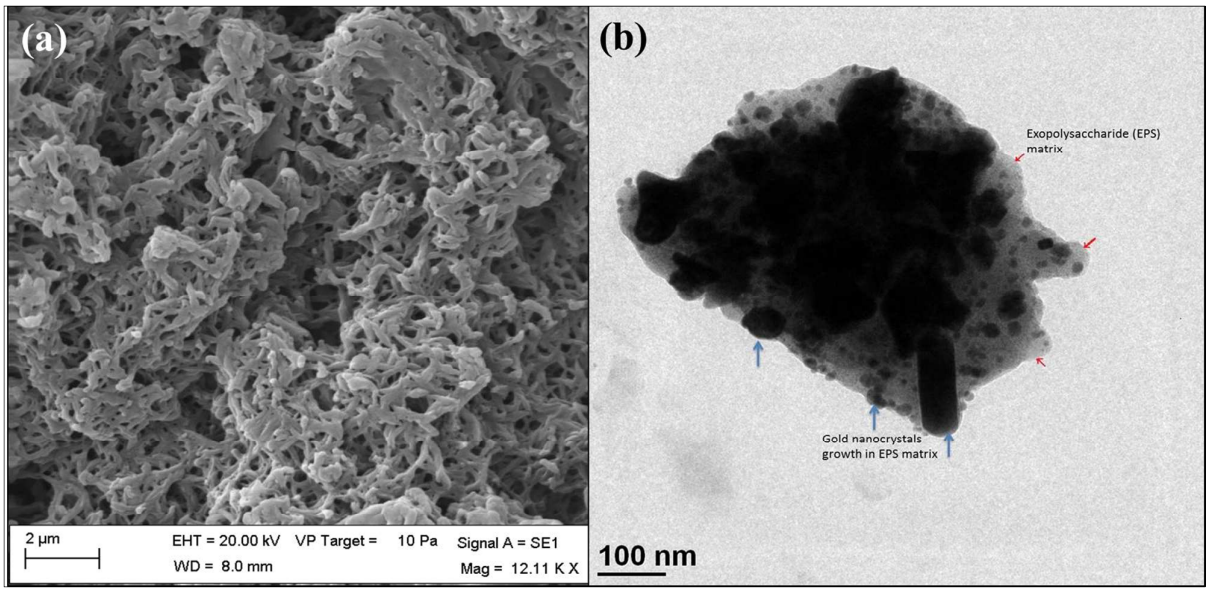

Fig. 6 Exopolysaccharide (EPS) and gold nanocrystals growth. (a) SEM image of EPS extracted from *Bacillus megaterium* MSBN04. (b) TEM image of EPS molecule packed with gold nanocrystals; growth of gold nanocrystals in massive exopolysaccharide (EPS) matrix.

548 **3.7 Antimicrobial activity of AuNPs**

549 The antimicrobial activity of AuNPs was tested against different pathogenic bacteria
550 (gram +ve & gram –ve) by well and disc diffusion method. The zone of inhibition around
551 each well and disc was measured and interpreted in Table 4. The highest antibacterial activity
552 was observed at the concentration of 100 µg/mL of AuNPs against *Klebsiella pneumoniae*
553 MTCC 432 followed by *E. coli* MTCC 78, *Bacillus cereus* MTCC 430, and *Pseudomonas*
554 *aeruginosa* CP1 in both well and disc diffusion method. The antibacterial activity of AuNPs
555 was highly comparable as that of Kim et al. (2008).[39] The AuNPs showed a broad spectrum
556 of activity which was similar to the results obtained from the AuNPs synthesized by plant-
557 based polysaccharides.[10, 12]

558

559 **Table 4** Antimicrobial activity of EPS based synthesized AuNPs. The antibacterial activity
560 of AuNPs was tested against pathogenic bacteria by well and disc diffusion method. The EPS
561 based AuNPs shows highest activity (inhibition zone -22 mm) towards *Klebsiella*
562 *pneumoniae* MTCC 432.

563

Test organisms	Pure EPS*		Chemically synthesized AuNPs*		EPS encrusted AuNPs*	
	Well	Disc	Well	Disc	Well	Disc
Staphylococcus aureus MTCC 98	2	3	9	11	8	5
Staphylococcus epidermidis MTCC 435	3	0	10	4	14	9
Klebsiella pneumoniae MTCC 432	4	1	13	8	22	17
Escherichia coli MTCC 78	2	0	6	4	17	14
Salmonella typhi MTCC 733	5	0	8	5	11	8
Bacillus cereus MTCC 430	1	2	5	7	16	12
Pseudomonas aeruginosa CP1	5	1	14	10	15	13
Vibrio cholerae CP2	3	0	17	11	12	9
Streptococcus pneumoniae CP3	0	0	8	5	5	2

564 * Inhibition zone in mm

EPS encrusted AuNPs show more inhibition against indicator organisms revealing the synergistic effect of EPS and AuNPs conjugate. Especially, EPS encrusted AuNPs expresses high inhibitory activity against *Klebsiella pneumoniae* (MTCC 432) than pure EPS and chemically synthesized AuNPs. Chemically synthesized AuNPs invariably limit their applicability in biomedical field but biogenic nanomaterials are considered as safe and more prominent agents in the field of nanomedicine. The advancement and application of nanomaterials as new antimicrobials should provide novel modes of action and/or different cellular targets compared with existing antibiotics.

4. Conclusions

A marine sponge-associated *Bacillus megaterium* MSBN04 was successfully used for the production of EPS. The green synthesis and stabilization method using bacterial EPS was developed for AuNPs preparation. Synthesis of the AuNPs was confirmed by UV-Vis spectroscopy and FT-IR. The TEM analysis shows that spherical AuNPs with mean diameter of 10 nm capped by a thin layer of EPS. The XRD spectrum of the EPS-stabilized AuNPs confirms the fabrication of crystalline gold. The prepared AuNPs were displays obvious antibacterial activity against test pathogens. The experimental results indicate that bacterial EPS is responsible for the synthesis and stabilization of AuNPs and these polysaccharide encrusted gold nanocrystals could be used for various nano-industrial and biological applications.

Acknowledgement

The authors would like to thank the anonymous reviewers for their valuable comments and suggestions to improve the quality of the paper. We thank Dr. R. Vijay Solomon, Swiss Federal Commission Fellow, Department of Chemistry, University of Basel, Switzerland for the critical reading of the manuscript.

590 **References**

591 1 B. Ismail and K. M. Nampoothiri, *Arch. Microbiol*., 2010, **192**, 1049.

592 2 C. Liu, J. Lu, L. Lu, Y. Liu, F. Wang and M. Xiao, *Bioresour. Technol.*, 2010, **101**, 5528.

593 3 G. Sathiyanarayanan, G. S. Kiran and J.Selvin, *Colloid. Surface. B.,* 2013, **102,** 13.

594 4 Z. Lin and H. Zhang, *Acta. Pharmacol. Sin.*, 2004, **25**, 1387.

595 5 I. A. Sutherland, *Microbiol. Today*, 2002, **29**, 70.

596 6 O. V. Salata, *J. Nanobiotechnol*., 2004, **2**, 3.

597 7 X. Zhou, J. M. E. Khoury, L. Qu, L. Dai and Q. Li, *J. Colloid. Interface. Sci.*, 2007, **308**,
598 381.

599 8 P. Mukherjee, M. Roy, B. P. Mandal, G. K. Dey, P. K. Mukherjee, J. Ghatak, A. K.
600 Tyagi and S. P. Kale, *Nanotechnol.*, 2008, **19**, 75103.

601 9 Y. N. Mata, E. Torres, M. L. Blázquez, A. Ballester, F. González and J. A. Muñoz, *J.*
602 *Hazard. Mater*., 2009, **166**, 612.

603 10 H. Huang and X. Yang, *Carbohydr. Res.*, 2004, **339**, 2627.

604 11 M. M. Kemp, A. Kumar, S. Mousa, T. J. Park, P. Ajayan, N. Kubotera, S. Mousa and R.
605 J. Linhardt, *Biomacromol.*, 2009, **10**, 589.

606 12 Y. Park, Y. N. Hong, A. Weyers, Y. S. Kim and R. J. Linhardt, *Nanobiotechnol*., 2011,
607 **5**, 69.

608 13 G. Sathiyanarayanan, G. S. Kiran, J. Selvin and G. Saibaba, *Int. J. Biol. Macromol*.,
609 2013, **60**, 253.

610 14 D. C. Montgomery, *Design and Analysis of Experiments*, Wiley: New York, 2001.

611 15 X. Wang, J. F. Preston and T. Romeo, *J. Bacteriol*., 2004, **186**, 2724.

612 16 M. Dubois, K. A. Gilles, J. K. Hamilton, P. A. Rebers and F. Smith, *Anal. Chem*., 1956,
613 **28**, 350.

614 17 M. M. Bradford, *Anal. Biochem*., 1976, **72**, 248.

18 T. T. Terho and K. Hartiala, *Anal. Biochem*., 1971, **41**, 471.

19 S. B. Deng, R. B. Bai, X. M. Hu and Q. Luo, *Appl. Microbiol. Biotechnol.*, 2003, **60**, 588.

20 R. P. Singh, M. K. Shukla, A. Mishra, P. Kumari, C. R. K. Reddy and B. Jha, *Carbohydr. Polym.*, 2011, **84**, 1019.

21 Y. Wang, C. Li, P. Liu, Z. Ahmed, P. Xiao and X. Bai, *Carbohydr. Polym.*, 2010, **82**, 895.

22 P. J. Bremer and G. G. Geesey, *Biofouling*, 1991, 3, 89.

23 S. Nataraj, R. Schomacker, M. Kraume, I. M. Mishra and A. Drews, *J. Membr. Sci.*, 2008, **308**, 152.

24 Z. Chi and S. Zhao, *Enzyme. Microbial. Technol*., 2003, **33**, 206.

25 G. H. Yu, P. J. He and L. M. Shao, *Bioresour. Technol*., 2009, **100**, 3193.

26 K. Fukuda, T. Shi, K. Nagami, F. Leo, T. Nakamura, K. Yasuda, A. Senda, H. Motoshima and T. Urashima, *Carbohydr. Polym*., 2009, **79**, 1040.

27 J. Koivukorpi, E. Sievänen, E. Kolehmainen and V. Král, *Molecules.,* 2007, ***12***, 13.

28 C. Ott, C. D. Easton, T. R. Gengenbach, S. L. McArthurb and P. A. Gunatillake, Polym. Chem., 2011, **2**, 2782.

29 D. -B. Mao, C. -W. Shi, J. -Y. Wu and C. -P. Xu, *Bioprocess. Biosyst. Eng*., 2013, DOI 10.1007/s00449-013-1111-3

30 Q. Ren, Y. Huang, H. Ma, F. Wang, J. Gao and J. Xu, BioResources., 2013, **8**, 1563.

31 R. P. Singh, T. Tripathy, G. P. Karmakar, S. K. Rath, N. C. Karmakar, S. R. Pandey, K. Kanan, S. K. Jain and N. T. Lan, *Curr. Sci.*, 2000, **78**, 798.

32 F. Freitas, V. D. Alves, M. Carvalheira, N. Costa, R. Oliveira, M. A. M. Reis, *Carbohydr. Polym.*, 2009, **78**, 549.

33 P. Kanmani and S. T. Lim, *Process. Biochem*., 2013, **48**, 1099.

34 X. Wang, C. E. Egan, M. Zhou, K. Prince, D. R. G. Mitchell and R. A. Caruso, *Chem. Commun*., 2007, **29**, 3060.

35 S. Li, Y. Shen, A. Xie, X. Yu, L. Qiu, L. Zhang and Q. Zhang, *Green. Chem*., 2007, **9**, 852.

36 B. Ankamwar, C. Damle, A. Ahmad and M. Sastry, *J. Nanosci. Nanotechnol*. 2005, **5**, 1665.

37 V. Vignesh, K. F. Anbarasi, S. Karthikeyeni, G. Sathiyanarayanan, P. Subramanian and R. Thirumurugan, *Colloids Surf. A.* 2013, **439**, 184.

38 H. Jang, Y. K. Kim, S. R. Ryoo, M. H. Kim and D. H. Min, *Chem. Commun*., 2010, **46**, 583.

39 K. J. Kim, W. S. Sung, S. K. Moon, J. S. Choi, J. G. Kim and D. G. Lee, *J. Microbiol. Biotechnol*., 2008, **18**, 1482.